Published in final edited form as:
Adv Funct Mater. 2009 December 9; 19(23): 3753–3759. doi:10.1002/adfm.200901253.

Porous Polymersomes with Encapsulated Gd-labeled Dendrimers as Highly Efficient MRI Contrast Agents**

Dr. Zhiliang Cheng
Department of Bioengineering, University of Pennsylvania 210 South 33rd Street, 240 Skirkanich Hall, Philadelphia, PA 19104 (USA)

Daniel L.J. Thorek
Department of Bioengineering, University of Pennsylvania 210 South 33rd Street, 240 Skirkanich Hall, Philadelphia, PA 19104 (USA)

Prof. Andrew Tsourkas*
Department of Bioengineering, University of Pennsylvania 210 South 33rd Street, 240 Skirkanich Hall, Philadelphia, PA 19104 (USA)

Abstract

The use of nanovesicles with encapsulated Gd as MR contrast agents has largely been ignored due to the detrimental effects of the slow water exchange rate through the vesicle bilayer on the relaxivity of encapsulated Gd. Here, we describe the facile synthesis of a composite MR contrast platform, consisting of dendrimer conjugates encapsulated in porous polymersomes. These nanoparticles exhibit improved permeability to water flux and a large capacity to store chelated Gd within the aqueous lumen, resulting in enhanced longitudinal relaxivity. The porous polymersomes, ~130 nm in diameter, were produced through the aqueous assembly of the polymers, polyethylene oxide-*b*-polybutadiene (PBdEO), and polyethylene oxide-*b*-polycaprolactone (PEOCL). Subsequent hydrolysis of the caprolactone (CL) block resulted in a highly permeable outer membrane. To prevent the leakage of small Gd-chelate through the pores, Gd was conjugated to PAMAM dendrimer via diethylenetriaminepentaacetic acid dianhydride (DTPA dianhydride) prior to encapsulation. As a result of the slower rotational correlation time of Gd-labeled dendrimers, the porous outer membrane of the nanovesicle, and the high Gd payload, these functional nanoparticles were found to exhibit a relaxivity (R1) of 292,109 mM^{-1} s^{-1} per particle. The polymersomes were also found to exhibit unique pharmacokinetics with a circulation half-life of >3.5 hrs and predominantly renal clearance.

Keywords

dendrimers; gadolinium; magnetic resonance; nanoparticles; polymersomes

1. Introduction

Magnetic resonance (MR) imaging has become well established as a powerful tool for diagnostic imaging, largely due to its ability to non-invasively acquire three-dimensional tomographic images with exquisite soft tissue contrast and anatomical detail. Many of these MR imaging procedures utilize non-targeted contrast agents such as gadolinium-

*atsourk@seas.upenn.edu.
**This work was supported in part by the National Institute of Health (NCI) R21 CA-125088, the American Cancer Society RSG-07-005-01, and the Transdisciplinary Program in Translational Medicine and Therapeutics. Supporting Information is available online from Wiley InterScience or from the author.

diethylenetriaminopentaacetic acid (i.e. Gd-DTPA).[1–5] These agents generally distribute into the intravascular and interstitial space and have been used to evaluate physiological parameters such as renal function and vascular permeability (e.g. rupture of the blood-brain barrier).[6–9] Dynamic contrast enhanced imaging has further extended the utility of gadolinium-based agents by providing insight into tissue pathologies. For example, malignant tumors are often associated with a faster increase in signal intensity than benign processes.[10]

More recently, gadolinium-based contrast agents have been engineered with diverse physical-chemical properties to encourage tissue specific accumulation. Biodistribution can be manipulated by either directly altering the chemical properties of the Gd-chelate, e.g. water-soluble Gd-complexes with a lipophilic moiety exhibit enhanced hepatic uptake, or by coupling chelated Gd to macromolecules or nanoparticles.[11–15] Gd-labeled (or loaded) nanoparticles have garnered a particularly high degree of interest. This is largely due to the ability of nanoparticles to carry a large payload of Gd, the ability to finely tune their physicochemical properties, which can influence their pharmacokinetic and pharmacodynamic profiles, and the ability to functionalize their surface with molecularly specific targeting agents.

Numerous nanoparticles have been explored as platforms for MR contrast agents, including dendrimers,[16] proteins,[17, 18] nanoemulsions,[19] solid nanoparticles,[20–22] and vesicles.[23–27] These agents have been used to improve the visualization of tumors,[28–30] atherosclerotic plaques,[31] lymph nodes,[32] inflammation sites,[33] and myocardium infarcted areas.[34] Among the many nanoparticulate systems that have been reported, hollow nanometer-sized vesicles are particularly attractive due to the increased functionality imparted by their amphiphilic structure. Specifically, hydrophilic compounds can be loaded in the aqueous lumen of the nanovesicles, the hydrophobic domain serves as a natural carrier environment for hydrophobic drugs, and the exterior surface can be functionalized with molecularly specific targeting ligands.

Nanovesicles have been transformed into effective paramagnetic contrast agents by either encapsulating chelated Gd within the aqueous lumen or by immobilizing the chelated Gd on the membrane surface. In general, the immobilization of chelated Gd on the surface of nanovesicles has become the preferred embodiment for MR imaging applications due to the detrimental effects of slow water exchange rate through the lipid bilayer on the relaxivity of Gd encapsulated within the lumen.[19, 24, 35, 36] For example, Gd-loaded liposomes that are 100 nm in diameter have been shown to exhibit a longitudinal relaxivity (R1) per Gd that is 62% lower than free chelated Gd.[23, 26] An additional advantage stemming from the attachment of chelated Gd to the nanovesicle surface is the enhancement in the R1 per Gd, which has been attributed to the slowed rotational correlation time, compared with free chelated Gd in solution.

Here, we re-explore the use of vesicles with encapsulated Gd as MR imaging agents. The foreseen advantage of loading chelated Gd within the intraparticle volume is the ability to achieve much higher Gd payloads, and thus higher relaxivities per particle, compared with nanovesicles that possess surface immobilized Gd. To overcome the slow water exchange across the membrane bilayer, highly `porous polymersomes' were adopted as the nanoparticulate carrier. Polymersomes represent a class of vesicles prepared from amphiphilic synthetic block copolymers that exhibit improved stability compared with liposomes.[37–40] We have previously shown that by increasing vesicle porosity, the relaxivity of encapsulated Gd can be restored.[41] Porosity was increased by incorporating phospholipids into the membrane of polymer nanovesicles, cross-linking the polymer and subsequently extracting the lipid. In this study an alternative poration technique was

employed that does not require polymer cross-linking, thus reducing the number of required synthesis and purification steps and also likely improving biodegradability. Specifically, porous polymersomes were formed through the aqueous assembly of the diblock copolymers, PEO(1300)-*b*-PBD(2500) (PBdEO) and PEO(2000)-*b*-PCL(2700) (PEOCL), followed by hydrolysis of the polycaprolactone block. Vesicles with similar composition have previously been used as platforms for drug delivery, whereby the caprolactone blocks were hydrolyzed upon acidification of the endosomal compartments and hydrophilic drugs were released through the newly formed pores.[42, 43] In this application, however, it was actually necessary to prevent the leakage of encapsulated Gd through the membrane pores. Therefore, the chelated Gd was bound to dendrimers prior to encapsulation. This also served to enhance the R1 per Gd, by slowing the rotational correlation time of the chelated Gd. Here, the design, assembly, characterization, biodistribution and circulation time of the paramagnetic porous polymersomes are discussed.

2. Results and Discussion

Porous polymersomes with encapsulated Gd-labeled dendrimer have been developed as MRI contrast agents, as shown schematically in Figure 1. The paramagnetic porous polymersomes were prepared by first encapsulating Gd-DTPA-labeled dendrimers into vesicles assembled from a mixture of two amphiphilic diblock copolymers, PBdEO and PEOCL, via thin film hydration. The mean diameter of the polymersomes was then reduced to 130 ± 10 nm (S.D.) by subjecting the sample to multiple freeze-thaw cycles and extrusion through a 100 nm polycarbonate filter (Fig. 2). The hydrodynamic diameter was determined by dynamic light scattering (DLS). For comparison, vesicles formed in the absence of dendrimers were also prepared and characterized by DLS (Fig. SI-1, Supporting Information). It was found that the addition of dendrimers did not seem to have a significant effect on polymersome size. When the extrusion pore size was changed to 80 nm, no significant reduction of vesicle diameter was observed. It is likely that the vesicle size could not be further reduced due to the energetic constraints imparted by the thick hydrophobic domain, ~10 nm. This is significantly larger than the hydrophobic domain of most liposomes, which are typically ~3 nm in thickness.[38] The improved structural stability of the polymersome bilayer architecture has made them an attractive alternative to liposomes, which are often limited in clinical applications by their low stability in circulation.[44]

The inclusion of PEOCL within the polymersome membrane allowed for the facile formation of pores via acid hydrolysis of the polycaprolactone block.[45] To confirm that pores were actually created, the fluorescent dye, carboxyfluorescein (CF), was entrapped within the aqueous lumen of the vesicles at self-quenching concentrations (i.e. 100 mM CF). The in situ release of CF was then monitored fluorometrically after incubating the polymersomes in acidic buffer (PBS, pH 5.1) at 37°C. It was found that polymersomes composed of 25 mol % PEOCL released more than 90% of the CF within four days (Fig. 3). In contrast, vesicles with 15 mol % PEOCL only exhibited 50 % release of CF over the same period. Vesicles formulated with 100 % PBdEO exhibited less than a 5 % release of the encapsulated dye over 4 days. These results confirm that the permeability/porosity of the polymersome can be increased by hydrolysis of the caprolactone polymer.

Since it is feasible that the formation of pores within the polymersome could lead to vesicle instability and collapse, the ability of the porous polymersome to retain its structure following PCL hydrolysis was examined. Specifically, the hydrodynamic diameter of the vesicles was measured by dynamic light scattering for 10 days following suspension of the polymersomes in PBS buffer (0.1 M phosphate, pH 5.1) at 37 °C. It was found that polymersomes prepared with 25 mol % PEOCL vesicles did not exhibit any significant change in hydrodynamic diameter and behaved similar to vesicles composed of 100 mol %

PBdEO (Fig. 4). It should be noted, however, that occasionally a small peak located at 30–40 nm was observed for vesicles containing PEOCL. This is thought to be due to the formation of micelles from partially hydrolyzed PEOCL copolymers that have been released from the polymersomes.

To further assess the structural integrity of the porous polymersomes, FITC-labeled dendrimer was encapsulated within the vesicle lumen and its release was quantified following suspension of the polymersomes in PBS buffer (0.1 M phosphate, pH 5.1) at 37°C. This assay was also used to evaluate whether or not incorporation of 25 mol % PEOCL into the polymersome membrane, and its subsequent hydrolysis, resulted in the formation of pores large enough to allow leakage of the Gd-labeled dendrimer. Release of the FITC-labeled dendrimer from the porous polymersomes was quantified by centrifuging the polymersome sample on a Microcon filtering device at various time points following suspension in acidic buffer and examining the flow-thru (i.e. diffusate) for fluorescence. It was previously confirmed that non-encapsulated FITC-labeled dendrimers (generation 3) could readily pass through the filter, while ~100 nm polymersomes could not. Therefore, it was expected that any dendrimer that was released from the polymersome would be detectable in the flow-thru, while encapsulated dendrimer would remain in the retentate. Consistent with the encapsulation of FITC-labeled dendrimers within structurally stable polymersomes, no significant increase in fluorescence was detected in the flow-thru for at least 5 days following suspension in acidic media (Fig. SI-2, Supporting Information). A similar assay was also conducted with polymersomes containing Gd-labeled dendrimers, whereby T1 measurements of the flow-thru were conducted to confirm the absence of Gd-labeled dendrimer. As expected, the T1 relaxation time of the flow-thru was similar to that of pure phosphate buffer, ~1000 ms.

To assess the loading efficiency and paramagnetic properties of porous polymersomes with encapsulated Gd-labeled dendrimers, inductively coupled plasma atomic emission spectroscopy (ICP-AES) was used to determine the amount of Gd within the polymersome sample. The relaxivity was then calculated as the slope of the curves 1/T1 vs. Gd concentration, as shown in Figure 5. It was found that the porous polymersomes, 130 nm in diameter, had an R1 relaxivity value of 7.5 mM^{-1} s^{-1} per Gd. For comparison, non-porous vesicles with Gd-labeled dendrimer encapsulated within the lumen had an R1 relaxivity of 3.4 mM^{-1} s^{-1} per Gd and non-porous vesicles with Gd-DTPA encapsulated within the lumen had an R1 of 1.7 mM^{-1} s^{-1} per Gd. Therefore, the generation of pores within the vesicle bilayer led to a 2.2-fold improvement in relaxivity per Gd and coupling of the Gd-DTPA to the dendrimer led to another 2-fold improvement in relaxivity. Combined, the paramagnetic porous polymersomes exhibited more than a 4.4-fold improvement in relaxivity per Gd compared with non-porous vesicles with encapsulated Gd-DTPA.

In addition to the enhancement observed in the relaxivity per Gd, paramagnetic porous polymersomes also benefit tremendously from their capacity to carry very large payloads of chelated Gd within their aqueous lumen. Specifically, it was estimated that there were 38,947 Gd per polymersome. This measurement assumed an average polymersome diameter of 130 nm and that no polymer was lost during the synthesis process, as described in materials and methods. The resultant relaxivity (R1) per porous polymersome is therefore 292,109 mM^{-1} s^{-1}. In comparison, Gd-DTPA possesses an R1 of only 3.9 mM^{-1} s^{-1}.

The paramagnetic properties of the polymersomes reported here compare very favorably with Gd-based agents that have previously been reported in the literature. For example, Gd-labeled shell-crosslinked nanoparticles (40 nm diameter) exhibit an R1 of 39 $mM^{-1}s^{-1}$ per Gd (0.47 T) but possess only 510 Gd per particle, which results in an R1 of 2×10^4 mM^{-1}

s^{-1} per nanoparticle.[36] This relaxivity is significantly lower than the paramagnetic porous polymersomes presented here.

Paramagnetic silica nanoparticles (~100 nm) have been found to exhibit an R1 of 9.0 mM^{-1} s^{-1} per Gd (4.7 T) and contain 16,000 Gd per nanoparticle, which results in an R1 of 1.4×10^5 mM^{-1} s^{-1} per nanoparticle.[46] While these properties are similar to those of the paramagnetic polymersomes, polymersomes possess a hydrophobic domain that presents a natural carrier environment for hydrophobic drugs. This may allow paramagnetic porous polymersomes to be more readily adapted for combined targeted drug delivery and MR imaging.

Perfluorocarbon nanoparticles have a reported R1 of 25.3 mM^{-1} s^{-1} per Gd (1.5 T) and 94,200 Gd per particle, which results in an R1 of 2.38×10^6 mM^{-1} s^{-1} per nanoparticle. Although this relaxivity is higher than that of the 130 nm polymersomes reported here, it should be noted that the perfluorocarbon particles are much larger with a diameter of 273 nm.[47] Further, scaling with volume, a porous polymersome of this size would possess 360,688 Gd and exhibit an R1 of 2.7×10^6 mM^{-1} s^{-1} per polymersome.

To assess the toxicity of the Gd-encapsulated polymersomes, various concentrations of the porous polymersome sample were incubated with NIH 3T3 fibroblasts and the metabolic activity of the cells was measured via an MTT assay. Each particle concentration was tested in triplicate. The data shown in Figure 6 indicate the cell viabilities normalized to a control cell sample that was not incubated with any polymersomes. In general, the polymersomes did not seem to have any significant effect on the viability of NIH 3T3 cells. In fact, no statistically significant difference in viability was observed even at a Gd concentration of 4.5 mM ($p > 0.05$).

The benign affect of the nanovesicle on cell viability led us to study the pharmacokinetics of the paramagnetic porous polymersomes in C57BL/6 mice. Measurement of Gd concentration within the blood at various time points following intravenous injection revealed a circulation half-life of >3.5 hrs (Fig. 7). This is considerably shorter than the half-life of analogous non-porous polymersomes, which exhibit a half-life of >15 hrs.[48] Further insight into the accelerated clearance of the porous polymersomes was obtained by acquiring T1-weighted magnetic resonance images just prior to intravenous injection of the polymersomes and 2, 4, and 24 hours post-injection (Fig. 8). It was found that there was a significant enhancement in signal in the kidneys at 2 hrs post-injection and in the bladder at 4 hrs, which is indicative of renal clearance. Quantification of the signal-to-noise showed a decrease in the signal enhancement in the kidneys and an increase in the spleen over the course of 24 hrs (Fig. SI-3, Supporting Information). Very little enhancement was observed in the liver over this same period. These measurements are consistent with post-mortem biodistribution data, which showed that <10% of the injected Gd dose was localized in the liver, even after 24 hrs (Fig. 9).

Interestingly, the biodistribution and MR-enhancement patterns observed with the Gd-encapsulated porous polymersomes are quite atypical for nanoparticles ~130 nm in diameter. Particles of this size generally show high levels of liver uptake with little renal clearance. Therefore, these data appear to indicate that the porous polymersomes are gradually destabilized in circulation resulting in the release of the Gd-DTPA-labeled dendrimer into the blood pool. Gd-DTPA-labeled dendrimers (G3) are known to undergo very rapid clearance by glomerular filtration (<30 minutes),[49–51] which can explain the MR signal enhancement observed in the kidney and the bladder. It should be noted that the significant difference in circulation time between the Gd-DTPA-labeled dendrimers alone

and those encapsulated within the porous polymersomes suggests that the polymersomes do not release their contents immediately after injection.

The unique pharmacokinetic properties of the paramagnetic porous polymersomes may make them a favorable option as either a blood pool agent or potentially even a targeted imaging agent, although targeting may require slightly longer circulation times to be effective. Currently, many large macromolecular complexes and nanoparticles are being evaluated as MR contrast agents, but their prolonged retention is often a major limitation for development towards clinical use.[49] It has previously been reported that uptake of gadolinium chloride in the liver could lead to the depletion of Kupffer cells, raising concerns about toxicity.[52, 53] Conversely, smaller MR contrast agents are rapidly excreted from the kidneys and thus only provide a small window for imaging and have fewer opportunities to bind target receptors, resulting in less accumulation at the target site. The porous polymersomes with encapsulated Gd-labeled dendrimers offer an extended circulation time compared with small MR contrast agents, but are still predominantly cleared by the kidney and thus likely to be more rapidly excreted from the body than conventional nanoparticles.

3. Conclusions

In conclusion, the preparation of porous polymersomes with encapsulated Gd-labeled dendrimers for magnetic resonance imaging applications has been described. The porous vesicle membrane leads to a significant improvement in the water-exchange rate of the encapsulated Gd due to the faster flux of water across the bilayer. When injected into living subjects, the gradual destabilization of the polymersomes allow the Gd-labeled dendrimers to be predominantly cleared by the kidneys, while still maintaining a relatively long circulation time of >3.5 hrs. This could provide an important advantage over other long-circulating MR contrast agents, which generally require metabolism of the contrast agent in the liver and exhibit prolonged retention in the body.

4. Experimental

Materials

PEO(1300)-*b*-PBD(2500) (PBdEO) and PEO(2000)-*b*-PCL (2700) were purchased from Polymer Source (Dorval, Quebec, Canada). PEO, PBD and PCL represent polyethylene oxide, polybutadiene, and polycaprolactone, respectively. PAMAM dendrimers (ethylenediamine core, generation 3) were from Aldrich Chemical Co. as 20% w/v solutions in methanol. 5-(and-6)-carboxyfluorescein (CF) and fluorescein isothiocyanate (FITC) were obtained from Molecular Probes. Diethylenetriaminepentaacetic acid dianhydride (DTPA dianhydride) and gadolinium (III) chloride were obtained from Sigma-Aldrich. All other chemicals were used as received. All of the buffer solutions were prepared with DI water.

Synthesis of PAMAM-DTPA-Gd

100 mg PAMAM was dissolved in 20 mL sodium bicarbonate buffer (0.1 M, pH 9.5) and reacted with 828 mg DTPA dianhydride. The reaction solutions were maintained at pH 9.5 with NaOH over the reaction time of 10 h. The PAMAM-DTPA was purified by centrifugal filter devices (Amicon Ultra-4, 5000 MWCO, Millipore Corp.). The purified PAMAM-DTPA conjugates were mixed with 240 mg $GdCl_3$ in 0.1 M citrate buffer (pH 5.6) for overnight at 42 °C. The unreacted Gd^{3+} was removed by centrifugal filter devices (Amicon Ultra-4, 5000 MWCO, Millipore Corp.) while simultaneously changing the buffer to 0.1 M PBS buffer. To ensure complete removal of unreacted Gd^{3+}, the Gd content in the eluent was checked after each centrifugation until no Gd^{3+} was detectable. The purified PAMAM-DTPA-Gd conjugates were used for vesicle encapsulation.

Preparation of Nanometer-Sized Vesicles

Polymer vesicles were prepared by dissolving PBdEO/PEOCL (100 mg PBdEO) in chloroform and then removing the solvent using a stream of N_2 gas. After further drying under vacuum overnight, the residual polymer film was hydrated with an aqueous solution (0.1 M PBS, pH 7.0) in a 65 °C water bath for half hour and then sonicated for another 1 hour at the same temperature. Samples were subjected to ten freeze-thaw-vortex cycles in liquid nitrogen and warm H_2O (65 °C), followed by extrusion 21 times through two stacked 100 nm Nuclepore polycarbonate filters using a stainless steel extruder (Avanti Polar Lipids). For dye encapsulation, 100 mM CF or 10 mg/mL PAMAM-FITC was added to the dried polymer films and freeze-thaw and extrusion were performed as described. Non-entrapped CF and PAMAM-FITC were removed via size exclusion chromatography using Sepharose CL-4B (Sigma-Aldrich) and rehydration buffer as the eluent. For PAMAM-DTPA-Gd encapsulation, PAMAM-DTPA-Gd was added to the dried polymer films. Non-entrapped PAMAM-DTPA-Gd was removed through repeated washing on centrifugal filter devices (Amicon Ultra-4, 100K MWCO, Millipore Corp.). To ensure complete removal of non-entrapped PAMAM-DTPA-Gd, the T1 relaxation time of the eluent was checked after each centrifugation until no Gd was detectable, i.e. until the T1-relaxation time was equivalent to that of sodium phosphate (pH 7.0) buffer (~1000 ms). T1-relaxation times were determined using a Bruker mq60 MR relaxometer operating at 1.41 T (60 MHz) and 40 °C.

Quantification of Gd Encapsulation

To determine the number of Gd per porous polymersome, it was assumed that none of the 100 mg of polymer was lost during the synthesis process. The number of polymersomes in the purified sample was then calculated by determining the amount of polymer in each vesicle. For this calculation, the average diameter of each polymersome was taken to be 130 nm. Further, the average area occupied by single polymer molecules in a bilayer has previously been determined to be ~1 nm^2, and the thickness of the polymersome bilayer has previously been determined to be ~10 nm. The amount of Gd in the polymersome sample was measured by ICP-AES.

Leakage assay

Measurements of the pH/temperature induced release of CF trapped within the vesicles were carried out as follows: 10 μL of CF-loaded vesicle suspension was added to 2 mL 0.1 M PBS buffer solution containing 100 mM NaCl and adjusted to pH 5.1. After the suspension was held at 37 °C for a given period, the fluorescence intensity at 525 nm was measured using an excitation of 490 nm. The amount of CF released (%) was calculated by means of equation (1)

$$\%\text{CF released} = (I_x - I_0) / (I_t - I_0) \times 100 \quad (1)$$

where I_0 is the fluorescence intensity of the vesicle suspension containing CF at the initial time, I_x is the fluorescence intensity at any given time, and I_t is the fluorescence intensity after addition of an aqueous solution of Triton X-100 to the suspension.

Cell culture

The NIH 3T3 mouse fibroblast cells (ATCC) were cultured in Dulbecco's Modified Eagle's medium with 10% fetal bovine serum at 37 °C under 5% CO_2. Cell viability via MTT assay. NIH 3T3 cells were seeded in 96-well plates at a density of 10, 000 cells per well. After incubation overnight (37 °C, 5% CO_2), the medium in each well was aspirated off and loaded with 100 μL of fresh medium containing nanoparticles with different Gd^{3+}

concentration. After incubation for 4 h, the nanoparticle containing medium in each well was aspirated off and replaced with 100 μL of medium and 10 μL of MTT reagent. The cells were incubated for 2 to 4 hours, then 100 μL detergent reagent was added and left at room temperature in the dark for 2 hours. The absorbance at 570 nm was measured using a microplate reader.

Biodistrubution Studies

Female C57BL/6 mice were obtained from Harlan Laboratories at 8-weeks of age and fed ad libitum. All experiments conformed to animal care protocols approved by the Institutional Animal Care and Use Committee (IACUC) of the University of Pennsylvania. Gd-containing porous vesicles were diluted with saline to a Gd concentration of 5 mM. Mice (n = 3 per time point, 2 time points) were anesthetized with 2% isoflurane and were injected via the tail vein. The injected volume per mouse was 200 μL. The mice were anesthetized prior to sacrifice at 4 and 24 hrs. Organs of interest were harvested and briefly washed in PBS. Both blood and organs were analyzed by the inductively coupled plasma mass spectrometry (ICP-MS). Additional animals were sacrificed at 2, 26, and 32 hours and the blood was collected and analyzed by ICP-MS to determine the half-life of Gd in circulation.

In vivo MR Imaging and Analysis

Imaging was performed using a 4.7 T small animal horizontal bore Varian INOVA system. Gradients used in the magnet were 12 cm diameter at 25 G/cm. Imaging was performed using a custom-built 50 mm diameter send-receive birdcage volume coil. Following induction of a mouse to the plane of anesthesia using 4% isoflurane/oxygen, mice were fixed to an acrylic patient bed in the prone position and maintained on a 1% isoflurane/oxygen mixture. Body temperature was monitored with a platinum rectal probe connected to a small-animal monitoring system (SA Incorporated) and maintained using a stream of heated air. T1-weighted images were acquired in the coronal plane using a spin-echo sequence with the following parameters; TR/TE = 500/16.98 milliseconds, matrix = 256 × 128, FOV = 80 × 40 mm, slice thickness = 1 mm, NEX = 4). Scans were completed prior to, 2, 4 and 24 hours after injection of polymersome at a Gd concentration of 5 mM. To determine signal to noise ratios, signal was measured from both kidneys or the spleen and divided by the background noise in three consecutive acquisition slices.

Instrumentation

Dynamic light scattering (DLS) measurements were performed on a Zetasizer Nano from Malvern Instruments. The scattering angle was held constant at 90°. The PBdEO concentration within vesicle sample for DLS measurement was 0.1 mg/mL. The diameter of the vesicle was determined from the CONTIN analysis of the intensity autocorrelation function. The displayed size data was intensity-weighted. Fluorescence spectra measurements were acquired on a SPEX FluoroMax-3 spectrofluorometer (Horiba Jobin Yvon). T1-relaxation times were determined using a Bruker mq60 MR relaxometer operating at 1.41 T (60 MHz). ICP-MS was performed from New Bolton Center (University of Pennsylvania). ICP-AES was performed by VHG Laboratories (Manchester, NH).

Supplementary Material

Refer to Web version on PubMed Central for supplementary material.

References

[1]. Wermuth PJ, Del Galdo F, Jimenez SA. Arthritis Rheum. 2009; 60:1508–1518. [PubMed: 19404939]

[2]. Huang SN, Liu C, Dai GP, Kim YR, Rosen BR. Neuroimage. 2009; 46:589–599. [PubMed: 19264139]

[3]. Kim S, Pickup S, Hsu O, Poptani H. NMR Biomed. 2009; 22:303–309. [PubMed: 19039800]

[4]. Knight RA, Karki K, Ewing JR, Divine GW, Fenstermacher JD, Patlak CS, Nagaraja TN. J. Cereb. Blood Flow Metab. 2009; 29:1048–1058. [PubMed: 19319145]

[5]. Lu HZ, Law M, Ge YL, Hesseltine SM, Rapalino O, Jensen JH, Helpern JA. NMR Biomed. 2008; 21:226–232. [PubMed: 17557363]

[6]. Caravan P, Ellison JJ, McMurry TJ, Lauffer RB. Chem. Rev. 1999; 99:2293–2352. [PubMed: 11749483]

[7]. Felix R, Schorner W, Laniado M, Niendorf HP, Claussen C, Fiegler W, Speck U. Radiology. 1985; 156:681–688. [PubMed: 4040643]

[8]. Lee DC, Klocke FJ. Curr. Cardiol. Rep. 2006; 8:59. [PubMed: 16507238]

[9]. Uematsu H, Maeda M. Eur. Radiol. 2006; 16:180–186. [PubMed: 16402258]

[10]. Su MY, Muhler A, Lao XY, Nalcioglu O. Magn. Reson. Med. 1998; 39:259–269. [PubMed: 9469709]

[11]. Pascolo L, Cupelli F, Anelli PL, Lorusso V, Visigalli M, Uggeri F, Tiribelli C. Biochem. Biophys. Res. Commun. 1999; 257:746–752. [PubMed: 10208854]

[12]. Bogdanov A, Weissleder R, Brady TJ. Adv. Drug Deliv. Rev. 1995; 16:335–348.

[13]. Hamm B, Staks T, Muhler A, Bollow M, Taupitz M, Frenzel T, Wolf KJ, Weinmann HJ, Lange L. Radiology. 1995; 195:785–792. [PubMed: 7754011]

[14]. Vogl TJ, Pegios W, McMahon C, Balzer J, Waitzinger J, Pirovano G, Lissner J. Am. J. Roentgenol. 1992; 158:887–892. [PubMed: 1546612]

[15]. giovagnoni A, Paci E. Magn. Reson. Imaging. Clin. N. Am. 1996; 4:61–72. [PubMed: 8673717]

[16]. Xu H, Regino CAS, Bernardo M, Koyama Y, Kobayashi H, Choyke PL, Brechbiel MW. J. Med. Chem. 2007; 50:3185–3193. [PubMed: 17552504]

[17]. Aime S, Frullano L, Crich SG. Angew. Chem.-Int. Edit. 2002; 41:1017–+.

[18]. Liepold L, Anderson S, Willits D, Oltrogge L, Frank JA, Douglas T, Young M. Magn. Reson. Med. 2007; 58:871–879. [PubMed: 17969126]

[19]. Morawski AM, Winter PM, Crowder KC, Caruthers SD, Fuhrhop RW, Scott MJ, Robertson JD, Abendschein DR, Lanza GM, Wickline SA. Magn. Reson. Med. 2004; 51:480–486. [PubMed: 15004788]

[20]. Gerion D, Herberg J, Bok R, Gjersing E, Ramon E, Maxwell R, Kurhanewicz J, Budinger TF, Gray JW, Shuman MA, Chen FF. J. Phys. Chem. C. 2007; 111:12542–12551.

[21]. Li IF, Su CH, Sheu HS, Chiu HC, Lo YW, Lin WT, Chen JH, Yeh CS. Adv. Funct. Mater. 2008; 18:766–776.

[22]. Rieter WJ, Taylor KML, An HY, Lin WL, Lin WB. J. Am. Chem. Soc. 2006; 128:9024–9025. [PubMed: 16834362]

[23]. Fossheim SL, Fahlvik AK, Klaveness J, Muller RN. Magn. Reson. Imaging. 1999; 17:83–89. [PubMed: 9888401]

[24]. Parac-Vogt TN, Kimpe K, Laurent S, Pierart C, Elst LV, Muller RN, Binnemans K. Eur. Biophys. J. Biophys. Lett. 2006; 35:136–144.

[25]. Tilcock C, Macdougall P, Unger E, Cardenas D, Fajardo L. Biochimica Et Biophysica Acta. 1990; 1022:181–186. [PubMed: 2306454]

[26]. Tilcock C, Unger E, Cullis P, Macdougall P. Radiology. 1989; 171:77–80. [PubMed: 2928549]

[27]. Unger E, Shen D, Wu GL, Fritz T. Magn. Reson. Med. 1991; 22:304–308. [PubMed: 1812361]

[28]. Bertini I, Bianchini F, Calorini L, Colagrande S, Fragai M, Franchi A, Gallo O, Gavazzi C, Luchinat C. Magn. Reson. Med. 2004; 52:669–672. [PubMed: 15334589]

[29]. Mulder WJM, Strijkers GJ, Habets JW, Bleeker EJW, van der Schaft DWJ, Storm G, Koning GA, Griffioen AW, Nicolay K. Faseb J. 2005; 19:2008–+. [PubMed: 16204353]

[30]. Sipkins DA, Cheresh DA, Kazemi MR, Nevin LM, Bednarski MD, Li KCP. Nat. Med. 1998; 4:623–626. [PubMed: 9585240]

[31]. Mulder WJM, Douma K, Koning GA, Van Zandvoort MA, Lutgens E, Daemen MJ, Nicolay K, Strijkers GJ. Magn. Reson. Med. 2006; 55:1170–1174. [PubMed: 16598732]

[32]. Trubetskoy VS, Cannillo JA, Milshtein A, Wolf GL, Torchilin VP. Magn. Reson. Imaging. 1995; 13:31–37. [PubMed: 7534860]

[33]. Sipkins DA, Gijbels K, Tropper FD, Bednarski M, Li KCP, Steinman L. J. Neuroimmunol. 2000; 104:1–9. [PubMed: 10683508]

[34]. Chu WJ, Simor T, Elgavish GA. NMR Biomed. 1997; 10:87–92. [PubMed: 9267866]

[35]. Amirbekian V, Lipinski MJ, Briley-Saebo KC, Amirbekian S, Aguinaldo JGS, Weinreb DB, Vucic E, Frias JC, Hyafil F, Mani V, Fisher EA, Fayad ZA. Proc. Natl. Acad. Sci. U. S. A. 2007; 104:961–966. [PubMed: 17215360]

[36]. Turner JL, Pan DPJ, Plummer R, Chen ZY, Whittaker AK, Wooley KL. Adv. Funct. Mater. 2005; 15:1248–1254.

[37]. Discher BM, Bermudez H, Hammer DA, Discher DE, Won YY, Bates FS. J. Phys. Chem. B. 2002; 106:2848–2854.

[38]. Discher BM, Won YY, Ege DS, Lee JCM, Bates FS, Discher DE, Hammer DA. Science. 1999; 284:1143–1146. [PubMed: 10325219]

[39]. Ghoroghchian PP, Frail PR, Susumu K, Blessington D, Brannan AK, Bates FS, Chance B, Hammer DA, Therien MJ. Proc. Natl. Acad. Sci. U. S. A. 2005; 102:2922–2927. [PubMed: 15708979]

[40]. Ghoroghchian PP, Frail PR, Susumu K, Park TH, Wu SP, Uyeda HT, Hammer DA, Therien MJ. J. Am. Chem. Soc. 2005; 127:15388–15390. [PubMed: 16262400]

[41]. Cheng ZL, Tsourkas A. Langmuir. 2008; 24:8169–8173. [PubMed: 18570445]

[42]. Ahmed F, Pakunlu RI, Brannan A, Bates F, Minko T, Discher DE. J. Control. Release. 2006; 116:150–158. [PubMed: 16942814]

[43]. Kim YH, Tewari M, Pajerowski JD, Cai SS, Sen S, Williams J, Sirsi S, Lutz G, Discher DE. J. Control. Release. 2009; 134:132–140. [PubMed: 19084037]

[44]. Immordino ML, Dosio F, Cattel L. Int. J. Nanomed. 2006; 1:297–315.

[45]. Shum HC, Kim JW, Weitz DA. J. Am. Chem. Soc. 2008; 130:9543–9549. [PubMed: 18576631]

[46]. Santra S, Bagwe RP, Dutta D, Stanley JT, Walter GA, Tan W, Moudgil BM, Mericle RA. Adv Mater. 2005; 17:2165–2169.

[47]. Morawski AM, Winter PM, Crowder KC, Caruthers SD, Fuhrhop RW, Scott MJ, Robertson JD, Abendschein DR, Lanza GM, Wickline SA. Magn Reson Med. 2004; 51:480–486. [PubMed: 15004788]

[48]. Photos PJ, Bacakova L, Discher B, Bates FS, Discher DE. J. Control. Release. 2003; 90:323–334. [PubMed: 12880699]

[49]. Kobayashi H, Kawamoto S, Jo SK, Bryant HL, Brechbiel MW, Star RA. Bioconjugate Chem. 2003; 14:388–394.

[50]. Langereis S, de Lussanet QG, van Genderen MHP, Meijer EW, Beets-Tan RGH, Griffioen AW, van Engelshoven JMA, Backes WH. NMR Biomed. 2006; 19:133–141. [PubMed: 16450331]

[51]. Sato N, Kobayashi H, Hiraga A, Saga T, Togashi K, Konishi J, Brechbiel MW. Magn. Reson. Med. 2001; 46:1169–1173. [PubMed: 11746584]

[52]. Hardonk MJ, Dijkhuis FWJ, Hulstaert CE, Koudstaal J. J. Leukoc. Biol. 1992; 52:296–302. [PubMed: 1522388]

[53]. Rai RM, Yang SQ, McClain C, Karp CL, Klein AS, Diehl AM. Am. J. Physiol.-Gastroint. Liver Physiol. 1996; 270:G909–G918.

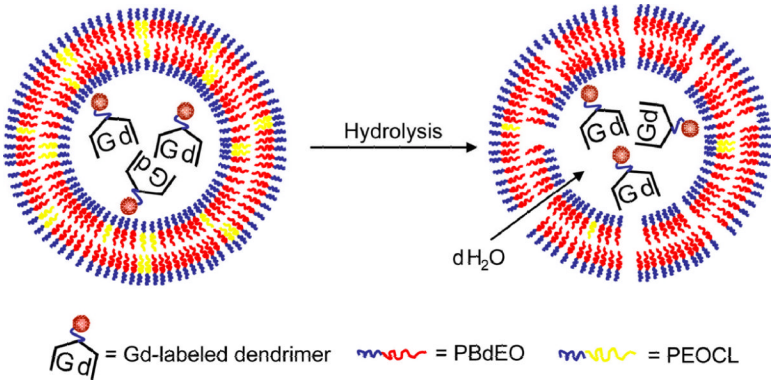

Figure 1.
Schematic diagram illustrating approach used to prepare paramagnetic porous vesicles. Nanovesicles were formed through the co-assembly of diblock inert copolymer PBdEO and biodegradable copolymer PEOCL. Gd-DTPA-labeled Generation 3 dendrimer were encapsulated within the aqueous interior during vesicle formation. Pores were subsequently formed in the polymersome bilayer by hydrolysis of the caprolactone block.

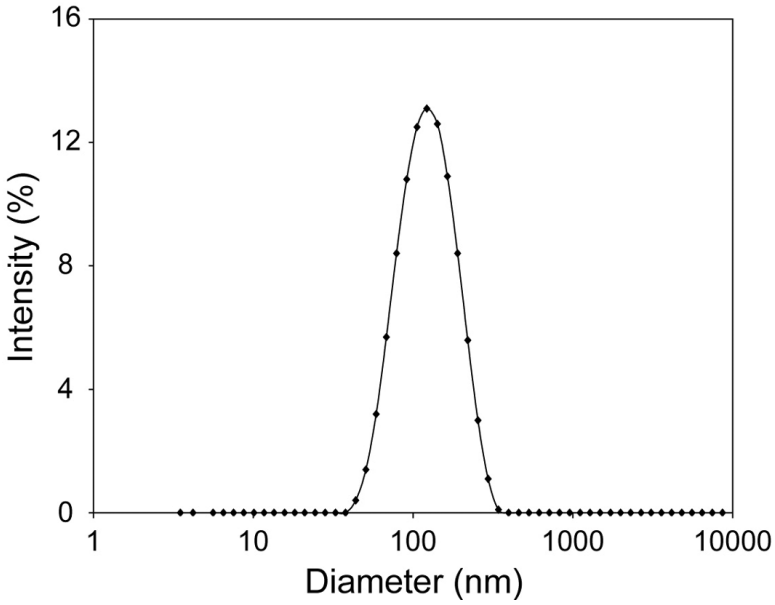

Figure 2.
Intensity-weighted hydrodynamic diameter of the extruded PBdEO/PEOCL vesicles (molar ratio, PBdEO:PEOCL = 75:25). Gd-labeled PAMAM (G3) was encapsulated within the aqueous lumen of vesicles. The measuring angle of DLS was 90 °.

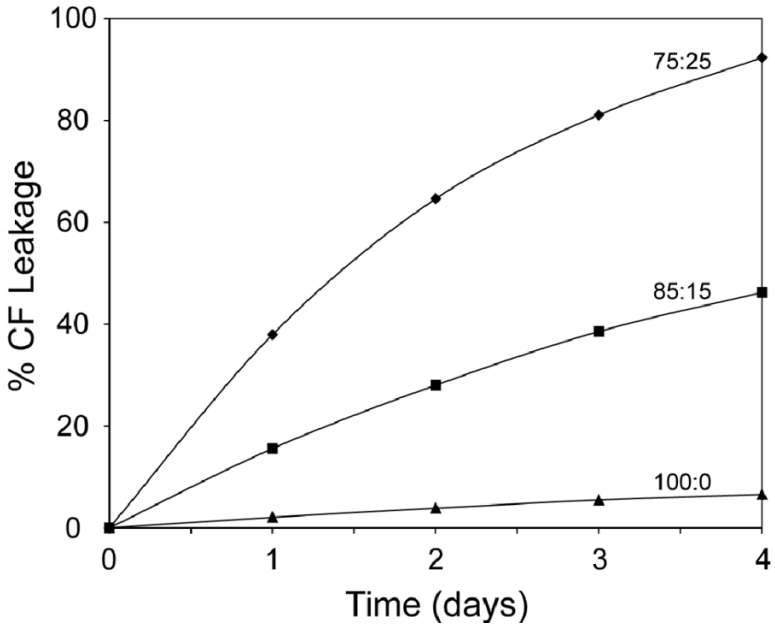

Figure 3.

Kinetics of CF release from nanovesicles prepared with PBdEO/PEOCL at molar ratios of (✦) 75: 25, (■) 85:15 and (▲) 100:0. The vesicles were incubated in PBS buffer (0.1 M, pH 5.1) and temperature 37 °C. At the end of each experiment, total CF fluorescence was determined by the addition Triton X-100.

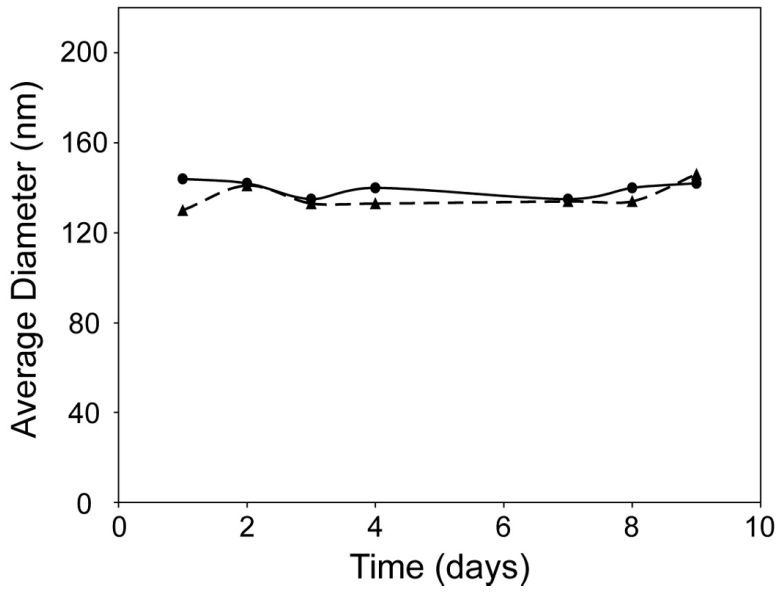

Figure 4.
Vesicle diameters as a function of storage time at PBS buffer (0.1 M, pH 5.1) and 37 °C. Vesicles prepared using PBdEO/PEOCL at a molar ratio of 75:25 (▲) and vesicles prepared from PBdEO only (•) were evaluated.

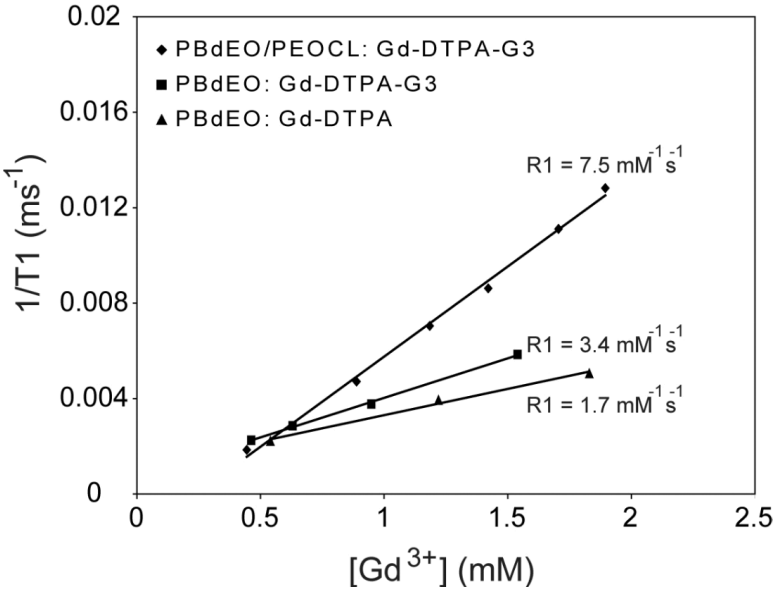

Figure 5.

Relaxivity determination for Gd-dendrimer conjugates encapsulated within porous polymersomes. Polymersomes were formed using 75%PBdEO and 25% PEOCL. This was followed by hydrolysis of the polycaprolactone block. T1 measurements were acquired at 1.41 T (60 MHz) at 40 °C. For comparison, T1 measurements were also made for Gddendrimer conjugates and Gd-DTPA encapsulated within non-porous PBdEO polymersomes.

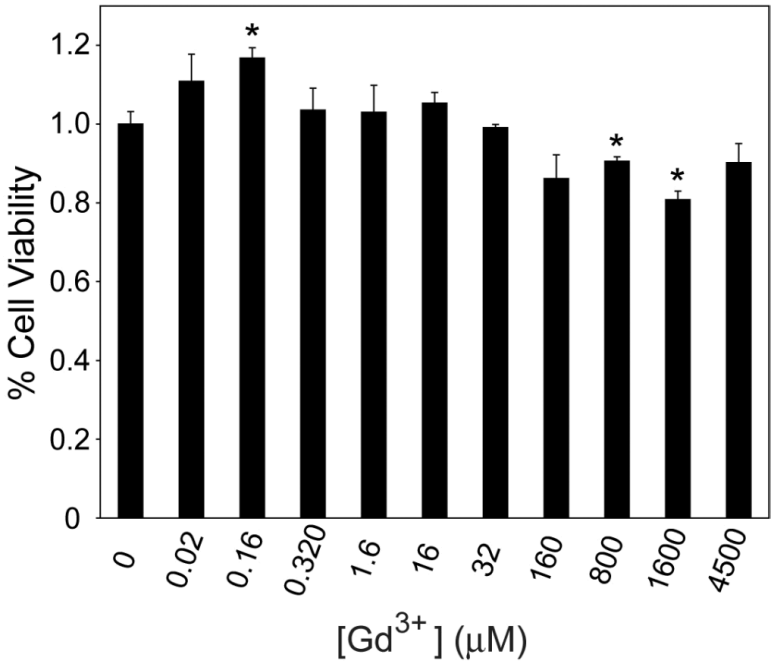

Figure 6.

The cell viability of NIH 3T3 cells incubated with nanovesicles. Nanovesicles were incubated with NIH 3T3 cells at various Gd concentrations for 4 hours. Viability was measured and normalized to cells grown in the absence of any particles based on MTT assay. The * represents statistical significant difference (t-test, two-tailed, unequal variance, $p < 0.05$) from 0 μM Gd concentration.

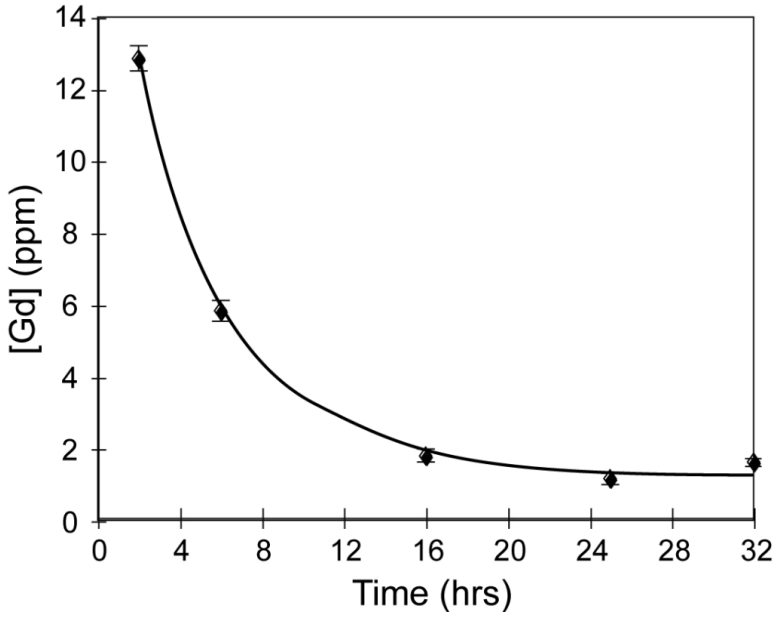

Figure 7.
Gd concentration in the blood at various times following the intravenous injection of Gd-encapsulated porous polymersomes into C57BL/6 mice.

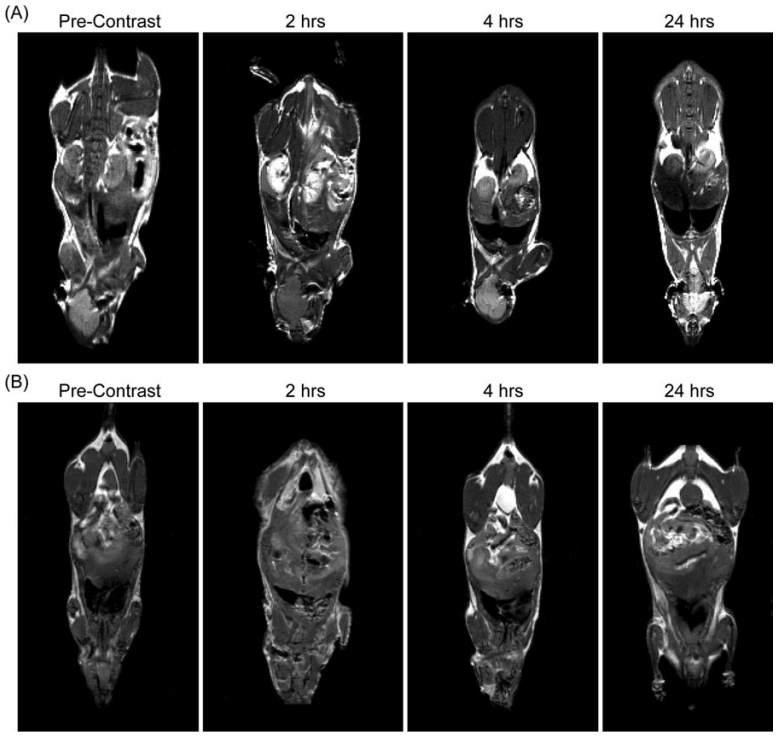

Figure 8.
Magnetic resonance images of C57BL/6 mice at various time points following the intravenous injection of Gd-encapsulated porous polymersomes. The local hyperintensity generated by the polymersoems was visualized using a 4.7 T small animal MR. Images of the (A) kidney and (B) bladder were acquired pre-injection and 2, 4 and 24 hr post-injection.

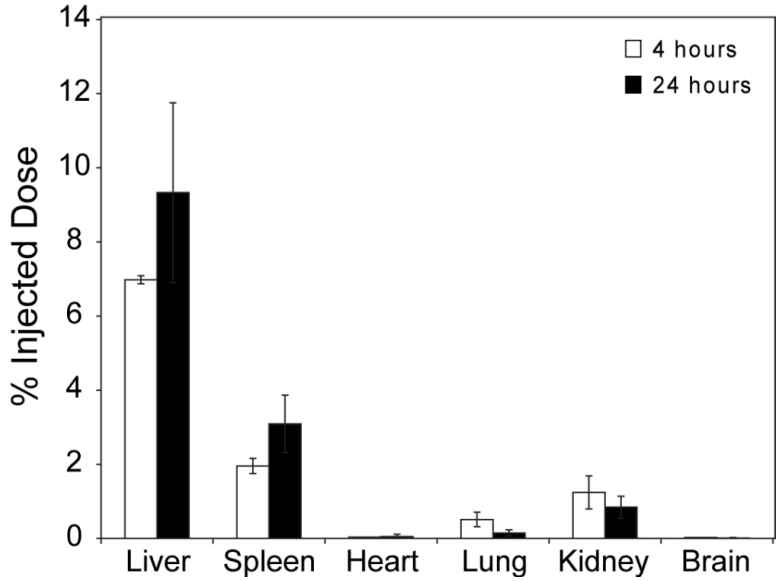

Figure 9.
Biodistribution of gadolinium in various organs isolated from C57BL/6 mice, 4 and 24 hrs after intravenous injection of Gd-encapsulated porous polymersomes. Gd content was quantified in each of the harvested organs by performing inductively coupled plasma mass spectroscopy (ICP-MS) (n = 3 per time point).